Title: Plant pathogenic fungi hijack phosphate starvation signaling with conserved enzymatic effectors

Authors: Carl L. McCombe[1]†, Alex Wegner[2]†, Chenie S. Zamora[3], Florencia Casanova[2], Shouvik Aditya[1], Julian R. Greenwood[1], Louisa Wirtz[2], Samuel de Paula[3], Eleanor England[1], Sascha Shang[1], Daniel J. Ericsson[4], Ely Oliveira-Garcia[3]*, Simon J. Williams[1]*, Ulrich Schaffrath[2]*

Affiliations:

[1]Research School of Biology, The Australian National University; Canberra, 2617, Australia.

[2]Department of Plant Physiology, RWTH Aachen University; Aachen, 52056, Germany.

[3]Department of Plant Pathology and Crop Physiology, Louisiana State University Agricultural Center; Baton Rouge, 70803, United States of America.

[4]ANSTO, Australian Synchrotron, Crystallography Beamline Group; Melbourne, 3168, Australia.

*Corresponding author. Email: schaffrath@bio3.rwth-aachen.de (U.S.); simon.williams@anu.edu.au (S.J.W.); EOliveiraGarcia@agcenter.lsu.edu (E.O.-G.)

† These authors contributed equally to this work.

Abstract: Phosphate availability modulates plant immune function and regulates interactions with beneficial, phosphate-providing, microbes. Here, we describe the hijacking of plant phosphate sensing by a family of Nudix hydrolase effectors from pathogenic *Magnaporthe oryzae* and *Colletotrichum* fungi. Structural and enzymatic analyses of the Nudix effector family demonstrate that they selectively hydrolyze inositol pyrophosphates, a molecule used by plants to monitor phosphate status and regulate starvation responses. In *M. oryzae*, gene deletion and complementation experiments reveal that the enzymatic activity of a Nudix effector significantly contributes to pathogen virulence. Further, we show that this conserved effector family induces phosphate starvation signaling in plants. Our study elucidates a molecular mechanism, utilized by multiple phytopathogenic fungi, that manipulates the highly conserved plant phosphate sensing pathway to exacerbate disease.

One-Sentence Summary: A family of conserved enzyme effectors from pathogenic fungi manipulate plant phosphate sensing to promote infection.

Main Text: Plant-microbe interactions range from beneficial to parasitic. Balancing the recruitment and support of symbiotic microbes, while maintaining the ability to defend against pathogens, is a major driver of plant evolution (*1*). The symbiosis between plants and arbuscular mycorrhizal fungi (AMF) predates the development of roots (*2*) and was likely instrumental in enabling land colonization by plants (*3*). Today, approximately 71% of vascular plants recruit AMF to access more phosphate and other mineral nutrients from the environment (*4*). In contrast to AMF, pathogenic fungi steal nutrients and constrain plant growth. Fungal diseases of important calorie crops threaten global food security by reducing crop yield (*5*). For example, *Magnaporthe oryzae* causes blast disease in major cereal crops including rice, wheat, and barley (*6*), resulting in annual food losses that could sustain hundreds of millions of people (*7*). Both symbiotic and pathogenic fungi secrete small proteins, called effectors, to optimize the host environment and support colonization.

Plant-AMF symbiosis is tightly regulated by the phosphate status of the plant (*8*). In eukaryotic cells, inositol pyrophosphates (PP-InsPs) signal phosphate availability through binding to SPX domains (*9*). When phosphate in plant cells is abundant, PP-InsP-bound SPX-domain proteins inhibit phosphate starvation response transcription factors (PHRs), thereby suppressing the expression of starvation induced genes (*10-13*). PHRs are conserved throughout land plants and green algae (*14*), and the regulation of plant-AMF symbiosis in both monocots and dicots is dependent on the PP-InsP/SPX/PHR signaling pathway (*15-18*). PHR activation also stimulates the expression of immune-suppressing genes and thereby inhibits the responsiveness of the plant immune system (*19,20*), indicating that plants prioritize symbiosis over defense during nutrient starvation. It is unknown whether any pathogenic fungi exploit the ancient and conserved phosphate-sensing pathway to promote plant infection. In this study, we demonstrate that a conserved family of Nudix (**Nu**cleoside-**di**phosphate linked to moiety-**X**) hydrolase effectors secreted by pathogenic fungi hydrolyze PP-InsPs. This function mimics phosphate depletion and hijacks the plant PHR signaling pathway. Gene deletion and complementation of *M. oryzae* Nudix effectors indicate that PP-InsP hydrolysis is essential for full virulence of the pathogen.

A conserved Nudix hydrolase effector family promotes blast disease

Pathogenic *Magnaporthe* and *Colletotrichum* fungi possess effectors with putative Nudix hydrolase activity (Fig. 1A and table S1) (*21*). There are three predicted Nudix effector genes in *M. oryzae* (table S1) (*22*); two of these, named *MoNUDIX*, are identical in sequence and are highly upregulated during infection (*23*). To examine the role of Nudix effectors in cereal blast disease, we first utilized RNA interference (RNAi) to simultaneously lower the expression of both identical *MoNUDIX* genes (fig. S1, A and B). Silencing of *MoNUDIX* reduced blast disease symptoms in whole rice plant spray inoculation assays (fig. S1C). Furthermore, we report that silencing *MoNUDIX* enhances reactive oxygen species (ROS) accumulation, slows disease progression, and increases cell-wall autofluorescence (fig. S1, D to G). Collectively, the results indicate that *MoNUDIX* is important for *M. oryzae* virulence and host immune suppression. To corroborate the RNAi results and further characterize the Nudix effectors, we generated *MoNUDIX* deletion and complementation mutants in *M. oryzae* utilizing CRISPR/Cas9 genome editing (fig. S2). The

deletion of both identical *MoNUDIX* gene copies (*M. oryzae*$^{\Delta\Delta MoNUDIX}$) resulted in a drastic reduction in rice blast lesion size (Fig. 1, B and C). To assess whether the contribution of MoNUDIX to blast virulence was specific to rice infection, we also performed infection assays with barley and again observed significantly reduced lesion size with *M. oryzae*$^{\Delta\Delta MoNUDIX}$ (Fig. 1, D and E). Our results were consistent across multiple rice and barley cultivars (Fig. 1, B and C, fig. S3, A and B), and microscopy analysis demonstrates a clear reduction in the growth of *M. oryzae*$^{\Delta\Delta MoNUDIX}$ running hyphae during infection (fig. S3C). The two identical *MoNUDIX* genes likely function redundantly, as single deletion mutants exhibit only slight reductions in disease symptoms when compared to wild-type *M. oryzae* (fig. S4, A and B). *M. oryzae*$^{\Delta\Delta MoNUDIX}$ displays normal vegetative growth, abiotic stress tolerance, conidia germination, appressorium formation, and infection following leaf wounding, which bypasses the requirement for an appressorium-mediated penetration (fig, S4, C to F). Collectively, our data indicate that MoNUDIX is important specifically for appressorium-mediated plant infection, this is consistent with the previously reported timing of Nudix effector gene induction during the late biotrophic growth stage of *M. oryzae, C. lentis,* and *C. higginsianum* (*21,23,24*).

Nudix hydrolases possess a conserved sequence motif, $GX_5EX_7REUXEEXGU$, where U represents a hydrophobic amino acid and X is any amino acid (*25*). The first glutamate and arginine form a stabilizing salt bridge, while the remaining glutamates often bind divalent metal co-factors essential for enzymatic activity. To investigate the importance of MoNUDIX Nudix hydrolase activity, *M. oryzae*$^{\Delta\Delta MoNUDIX}$ was complemented with either the wild-type effector, or effectors with various substitution mutations in the Nudix sequence motif. The expression of wild-type *MoNUDIX* successfully rescued the virulence of *M. oryzae*$^{\Delta\Delta MoNUDIX}$, whereas expression of the mutant effector genes did not (Fig. 1, D to F). These data demonstrate that the Nudix motif and therefore hydrolytic activity is essential for the promotion of blast disease by MoNUDIX.

Magnaporthe and *Colletotrichum* Nudix effectors are diphosphoinositol polyphosphate phosphohydrolases

Nudix hydrolases typically hydrolyze pyrophosphate bonds in molecules with a nucleoside diphosphate. To characterize the enzymatic activity and substrate specificity of the Nudix effectors, we determined the crystal structure of MoNUDIX. Structural similarity searches revealed that *Homo sapiens* diphosphoinositol polyphosphate phosphohydrolase 1 (*Hs*DIPP1) is remarkably similar to MoNUDIX in both overall structure and surface charge properties (Fig. 2A). *Hs*DIPP1, a well-characterized Nudix hydrolase, hydrolyzes diadenosine polyphosphates (Ap_nAs) (*26*), the protective 5′ mRNA cap (*27*), and PP-InsPs (*28*). Substrate screening with purified MoNUDIX protein demonstrated Nudix motif-dependent hydrolysis of 5-PP-$InsP_5$ (Fig. 2B), while no activity was detected with Ap_nAs, mRNA caps, or other common substrates of Nudix hydrolases (fig. S5, A and B). Our results demonstrate that MoNUDIX is a selective diphosphoinositol polyphosphate phosphohydrolase *in vitro*. To understand the mode of PP-InsP binding to MoNUDIX, we modelled 5-PP-$InsP_5$ into the MoNUDIX crystal structure via alignment with substrate bound *Hs*DIPP1 (*29*) (Fig. 2C). We identified basic amino acids likely required for PP-InsP binding (Fig. 2C); to confirm their involvement two lysines were mutated to glutamate

(MoNUDIX^{KKEE}). The MoNUDIX^{KKEE} protein demonstrated an approximately 70-fold reduction in inositol hexakisphosphate ($InsP_6$) binding affinity as measured by micro-scale thermophoresis (fig. S5C) and was unable to hydrolyze 5-PP-$InsP_5$ (Fig. 2D). The predicted PP-InsP binding site, including the basic amino acids, are conserved throughout the *Magnaporthe* and *Colletotrichum* Nudix effector family (Fig. 2, E and F), suggesting the conservation of substrate selectivity and enzymatic activity. To test this, we purified two homologs of MoNUDIX, one from *C. higginsianum* (ChNUDIX) and a second predicted *M. oryzae* Nudix effector (MoNUDIX2). Both ChNUDIX and MoNUDIX2 hydrolyze 5-PP-$InsP_5$ and this activity is dependent on a Nudix motif glutamate (Fig. 2G). Conversely, AvrM14, a sequence-unrelated mRNA decapping Nudix hydrolase effector from the fungus *Melampsora lini* (*30*), does not hydrolyze 5-PP-$InsP_5$ (fig S5D). All Nudix effectors used throughout this study were purified to homogeneity prior to *in vitro* characterization (fig. S6). Overall, structural analysis and enzymatic assays reveal that the *Magnaporthe* and *Colletotrichum* Nudix effectors are diphosphoinositol polyphosphate phosphohydrolases.

MoNUDIX localizes in the host cell cytoplasm during plant infection

Magnaporthe oryzae effectors can function within the host plant cell, or in the apoplastic space between the fungal cell wall and plant plasma membrane. The proteins involved in PP-InsP metabolism and signaling are intracellular. We therefore hypothesized that the Nudix effector family would function within the host plant cell during infection. We sought to identify the localization of MoNUDIX during plant infection using live-cell imaging techniques. First, we transformed *M. oryzae* with mRFP-tagged MoNUDIX controlled by the native promoter and determined that the effector co-localizes with the known cytoplasmic effector *Mo*Pwl2 in the biotrophic interfacial complex (BIC) (Fig. 3A). Using the native promoter was required for BIC localization, constitutive expression of MoNUDIX resulted in localization throughout the fungal hyphae (fig. S7). The BIC is the site of cytoplasmic effector translocation from the fungus into the host cell (*31*, *32*), therefore our data suggest that MoNUDIX is a cytoplasmic effector. Treatment with brefeldin A (BFA), a potent inhibitor of Golgi trafficking (*33*), prevents the secretion of apoplastic but not cytoplasmic *M. oryzae* effectors (*32*). We demonstrate that the BIC localization of MoNUDIX is not influenced by BFA treatment, further indicating that MoNUDIX functions as a cytoplasmic effector (Fig. 3B). For concentration of cytoplasmic fluorescence and verification of MoNUDIX localization in the host cell cytoplasm, we utilized a gentle plasmolysis procedure. The MoNUDIX:mRFP signal is clearly observed in the host plant cell protoplasts following treatment with KNO_3 (Fig. 3C). Overall, our results demonstrate that MoNUDIX localizes within the host cell cytoplasm during plant infection.

The Nudix effector family activates plant phosphate starvation responses

A reduction in intracellular PP-InsP concentration, as occurs when phosphate is limited, leads to the activation of PHRs and phosphate starvation responses (PSRs). The depletion of PP-InsPs due to hydrolysis by the Nudix effectors should mimic localized phosphate starvation (fig. S8A). To determine if the Nudix effectors activate PHRs and PSRs in plants, we transiently expressed MoNUDIX, ChNUDIX, and mutated proteins without enzymatic activity (MoNUDIX^{E79Q} and

ChNUDIX^{E78Q}) in *Nicotiana benthamiana*. We selected two phosphate starvation induced (PSI) genes, *Nb*SPX1 and *Nb*PECP1, for gene expression analysis (*34*, *35*). Both *Nb*SPX1 and *Nb*PECP1 have multiple PHR1-binding sequence (P1BS) elements in their promoter regions (fig. S8B). MoNUDIX and ChNUDIX significantly increased the abundance of *Nb*SPX1 and *Nb*PECP1 mRNA, when compared to MoNUDIX^{E79Q}, ChNUDIX^{E78Q}, and a no effector protein control (Fig. 4A). To investigate this further, we developed a rapid *in planta* screening method to monitor PHR activation. In our system, the RUBY reporter gene is controlled by a synthetic promoter with multiple P1BS elements, we named the promoter/reporter construct PSI:RUBY (fig. S8C). This system allowed us to screen six Nudix effector family members along with their corresponding Nudix motif mutants and other negative controls (nanoluciferase and AvrM14). We report that all six Nudix effectors significantly increase the expression of the RUBY reporter when compared to the corresponding Nudix motif mutant proteins and the negative controls (Fig. 4, B and C). Additionally, MoNUDIX^{KKEE} expression results in reduced RUBY expression when compared to wild-type MoNUDIX, consistent with the reduced $InsP_6$ binding and a lack of 5-PP-$InsP_5$ hydrolysis observed *in vitro* (Fig. 4, B and C). We also observe similar results when swapping the synthetic P1BS promoter with the 1 kb promoter region from *Nb*PECP1 (fig. S8, D and E). For all proteins, accumulation in *N. benthamiana* leaf tissue was detected via immunoblotting (fig. S8F). Collectively, our data demonstrate that the enzymatic activity of the Nudix effectors activates PHRs and PSI gene expression in *N. benthamiana*.

To determine if MoNUDIX induces PSRs during rice infection, we compared the mRNA levels of two PSI rice genes (*Os*SPX1 and *Os*IPS2) in two different rice cultivars throughout the infection process with either wild-type *M. oryzae* or *M. oryzae* $^{\Delta\Delta MoNUDIX}$. At 72 hours post inoculation the expression of both *Os*SPX1 and *Os*IPS2 is significantly upregulated in rice infected with wild-type MoNUDIX when compared to *M. oryzae* $^{\Delta\Delta MoNUDIX}$, suggesting that MoNUDIX promotes the expression of PSI genes in rice (Fig. 4D).

In *A. thaliana*, phosphate starvation induces the expression of immunosuppressant rapid alkalization factor (RALF) genes with P1BS elements in their promoter region (for example *At*RALF23) (*20*, *36*). This reduces reactive oxygen species (ROS) production triggered by immune elicitors (*20*, *36*). Similarly, in *N. benthamiana* the enzymatic activity of the Nudix effectors induces the expression of an *At*RALF23 homolog (designated *Nb*RALF23) and prevents the immune-activated ROS burst (Fig. 4, E and F). Overall, our results demonstrate that the diphosphoinositol polyphosphate phosphohydrolase effectors can activate phosphate starvation responses, which likely results in the suppression of plant immunity.

Discussion and conclusion

Phosphate is an essential but often limiting nutrient for plant growth, with phosphate-starved plants actively recruiting soil microbes to improve phosphate acquisition. Plant phosphate status is important for the regulation of multiple plant-microbe interactions (*37-42*). Here, we describe the molecular basis for phosphate status manipulation by pathogenic fungi. Our findings provide direct evidence for the hijacking of symbiosis-facilitating mechanisms by pathogenic fungi to promote disease.

The deletion of *MoNUDIX* genes in *M. oryzae* resulted in impaired plant colonization and fungal growth. The infection phenotype of *M. oryzae*$^{\Delta\Delta MoNUDIX}$ is analogous to phr2-mutant rice inoculated with AMF (*17*) and suggests that PHR-activation can enhance both beneficial and pathogenic infection in rice. Like AMF, *Colletotrichum tofieldiae* promotes host plant growth by providing phosphate under starvation conditions (*38*). We were unable to identify Nudix effectors in *C. tofieldiae*, and their absence may be required to ensure *C. tofieldiae* growth remains appropriately regulated by plant phosphate status. Conversely, multiple pathogenic *Colletotrichum* species have Nudix effectors that we demonstrate activate starvation responses. Three *C. higginsianum* Nudix effectors (two copies of *ChNUDIX*, one copy of *ChNUDIX2*) are clustered together on a mini-chromosome (chromosome 11) and are highly upregulated early in plant infection (*24*). Similar to *M. oryzae*$^{\Delta\Delta MoNUDIX}$, C. *higginsianum* mutants lacking chromosome 11 display normal vegetative growth and can successfully penetrate host plant cells but demonstrate inhibited disease progression (*43*). There are only 8 predicted effector genes on chromosome 11 (*44*), and therefore it is likely that Nudix effectors are also important for the pathogenicity of *C. higginsianum*.

In addition to their central role in phosphate homeostasis, PP-InsPs are co-factors for the receptors sensing the phytohormones auxin and jasmonate (*45-48*). Phosphate status and jasmonate signaling are intricately linked in plants. For example, jasmonate treatment stimulates PP-InsP synthesis (*49*), and PHR-activation enhances jasmonate production and signaling (*50*, *51*). By manipulating intracellular PP-InsP levels, the Nudix effectors may influence jasmonate and auxin signaling in their host plants in addition to inducing starvation responses.

Based on our data, we propose the following model describing the function of the *Magnaporthe* and *Colletotrichum* Nudix hydrolase effector family (Fig. 5). First, the effectors are translocated into their respective host plant cells. Once inside, they function as PP-InsP hydrolase enzymes, effectively uncoupling PHR activation from intracellular phosphate availability. This induces a plethora of transcriptional changes to promote phosphate acquisition and suppress immune responses, ultimately promoting disease.

References and Notes

1. P. M. Delaux, S. Schornack, Plant evolution driven by interactions with symbiotic and pathogenic microbes. *Science* **371**, 934-939 (2021).
2. M. C. Brundrett, Coevolution of roots and mycorrhizas of land plants. *New Phytol.* **154**, 275-304 (2002).
3. M. Parniske, Arbuscular mycorrhiza: the mother of plant root endosymbioses. *Nat. Rev. Microbiol.* **6**, 763-775 (2008).
4. M. C. Brundrett, L. Tedersoo, Evolutionary history of mycorrhizal symbioses and global host plant diversity. *New Phytol.* **220**, 1108-1115 (2018).
5. E. Stukenbrock, S. Gurr, Address the growing urgency of fungal disease in crops. *Nature* **617**, 31-34 (2023).
6. N. J. Talbot, On the trail of a cereal killer: Exploring the biology of Magnaporthe grisea. *Annu Rev Microbiol.* **57**, 177-202 (2003).
7. M. C. Fisher, D. A. Henk, C. J. Briggs, J. S. Brownstein, L. C. Madoff, S. L. McCraw, S. J. Gurr, Emerging fungal threats to animal, plant and ecosystem health. *Nature* **484**, 186-194 (2012).
8. L. M. Müller, M. J. Harrison, Phytohormones, miRNAs, and peptide signals integrate plant phosphorus status with arbuscular mycorrhizal symbiosis. *Curr. Opin. Plant Biol.* **50**, 132-139 (2019).
9. R. Wild, R. Gerasimaite, J.-Y. Jung, V. Truffault, I. Pavlovic, A. Schmidt, A. Saiardi, H. J. Jessen, Y. Poirier, M. Hothorn, A. Mayer, Control of eukaryotic phosphate homeostasis by inositol polyphosphate sensor domains. *Science* **352**, 986-990 (2016).
10. M. K. Ried, R. Wild, J. Zhu, J. Pipercevic, K. Sturm, L. Broger, R. K. Harmel, L. A. Abriata, L. A. Hothorn, D. Fiedler, S. Hiller, M. Hothorn, Inositol pyrophosphates promote the interaction of SPX domains with the coiled-coil motif of PHR transcription factors to regulate plant phosphate homeostasis. *Nat. Commun.* **12**, 384 (2021).
11. Z. Guan, Q. Zhang, Z. Zhang, J. Zuo, J. Chen, R. Liu, J. Savarin, L. Broger, P. Cheng, Q. Wang, K. Pei, D. Zhang, T. Zou, J. Yan, P. Yin, M. Hothorn, Z. Liu, Mechanistic insights into the regulation of plant phosphate homeostasis by the rice SPX2 - PHR2 complex. *Nat. Commun.* **13**, 1581 (2022).
12. J. Dong, G. Ma, L. Sui, M. Wei, V. Satheesh, R. Zhang, S. Ge, J. Li, T. E. Zhang, C. Wittwer, H. J. Jessen, H. Zhang, G. Y. An, D. Y. Chao, D. Liu, M. Lei, Inositol Pyrophosphate $InsP_8$ Acts as an Intracellular Phosphate Signal in Arabidopsis. *Mol. Plant* **12**, 1463-1473 (2019).
13. J. Zhu, K. Lau, R. Puschmann, R. K. Harmel, Y. Zhang, V. Pries, P. Gaugler, L. Broger, A. K. Dutta, H. J. Jessen, G. Schaaf, A. R. Fernie, L. A. Hothorn, D. Fiedler, M. Hothorn, Two bifunctional inositol pyrophosphate kinases/phosphatases control plant phosphate homeostasis. *eLife* **8**, e43582 (2019).
14. V. Rubio, F. Linhares, R. Solano, A. C. Martín, J. Iglesias, A. Leyva, J. Paz-Ares, A conserved MYB transcription factor involved in phosphate starvation signaling both in vascular plants and in unicellular algae. *Genes Dev.* **15**, 2122-2133 (2001).
15. P. Wang, R. Snijders, W. Kohlen, J. Liu, T. Bisseling, E. Limpens, Medicago SPX1 and SPX3 regulate phosphate homeostasis, mycorrhizal colonization, and arbuscule degradation. *Plant Cell* **33**, 3470-3486 (2021).
16. D. Liao, C. Sun, H. Liang, Y. Wang, X. Bian, C. Dong, X. Niu, M. Yang, G. Xu, A. Chen, S. Wu, SlSPX1-SlPHR complexes mediate the suppression of arbuscular mycorrhizal symbiosis by phosphate repletion in tomato. *Plant Cell* **34**, 4045-4065 (2022).
17. D. Das, M. Paries, K. Hobecker, M. Gigl, C. Dawid, H. M. Lam, J. Zhang, M. Chen, C. Gutjahr, PHOSPHATE STARVATION RESPONSE transcription factors enable arbuscular mycorrhiza symbiosis. *Nat. Commun.* **13**, 477 (2022).
18. J. Shi, B. Zhao, S. Zheng, X. Zhang, X. Wang, W. Dong, Q. Xie, G. Wang, Y. Xiao, F. Chen, N. Yu, E. Wang, A phosphate starvation response-centered network regulates mycorrhizal symbiosis. *Cell* **184**, 5527-5540 e5518 (2021).
19. G. Castrillo, P. J. Teixeira, S. H. Paredes, T. F. Law, L. de Lorenzo, M. E. Feltcher, O. M. Finkel, N. W. Breakfield, P. Mieczkowski, C. D. Jones, J. Paz-Ares, J. L. Dangl, Root microbiota drive direct integration of phosphate stress and immunity. *Nature* **543**, 513-518 (2017).
20. J. Tang, D. Wu, X. Li, L. Wang, L. Xu, Y. Zhang, F. Xu, H. Liu, Q. Xie, S. Dai, D. Coleman-Derr, S. Zhu, F. Yu, Plant immunity suppression via PHR1-RALF-FERONIA shapes the root microbiome to alleviate phosphate starvation. *EMBO J.* **41**, e109102 (2022).
21. V. Bhadauria, S. Banniza, A. Vandenberg, G. Selvaraj, Y. Wei, Overexpression of a novel biotrophy-specific Colletotrichum truncatum effector, CtNUDIX, in hemibiotrophic fungal phytopathogens causes incompatibility with their host plants. *Eukaryot Cell* **12**, 2-11 (2013).

22. R. A. Dean, N. J. Talbot, D. J. Ebbole, M. L. Farman, T. K. Mitchell, M. J. Orbach, M. Thon, R. Kulkarni, J. R. Xu, H. Pan, N. D. Read, Y. H. Lee, I. Carbone, D. Brown, Y. Y. Oh, N. Donofrio, J. S. Jeong, D. M. Soanes, S. Djonovic, E. Kolomiets, C. Rehmeyer, W. Li, M. Harding, S. Kim, M. H. Lebrun, H. Bohnert, S. Coughlan, J. Butler, S. Calvo, L. J. Ma, R. Nicol, S. Purcell, C. Nusbaum, J. E. Galagan, B. W. Birren, The genome sequence of the rice blast fungus Magnaporthe grisea. *Nature* **434**, 980-986 (2005).
23. X. Yan, B. Tang, L. S. Ryder, D. MacLean, V. M. Were, A. B. Eseola, N. Cruz-Mireles, W. Ma, A. J. Foster, M. Osés-Ruiz, N. J. Talbot, The transcriptional landscape of plant infection by the rice blast fungus Magnaporthe oryzae reveals distinct families of temporally co-regulated and structurally conserved effectors. *Plant Cell* **35**, 1360-1385 (2023).
24. R. J. O'Connell, M. R. Thon, S. Hacquard, S. G. Amyotte, J. Kleemann, M. F. Torres, U. Damm, E. A. Buiate, L. Epstein, N. Alkan, J. Altmüller, L. Alvarado-Balderrama, C. A. Bauser, C. Becker, B. W. Birren, Z. Chen, J. Choi, J. A. Crouch, J. P. Duvick, M. A. Farman, P. Gan, D. Heiman, B. Henrissat, R. J. Howard, M. Kabbage, C. Koch, B. Kracher, Y. Kubo, A. D. Law, M. H. Lebrun, Y. H. Lee, I. Miyara, N. Moore, U. Neumann, K. Nordström, D. G. Panaccione, R. Panstruga, M. Place, R. H. Proctor, D. Prusky, G. Rech, R. Reinhardt, J. A. Rollins, S. Rounsley, C. L. Schardl, D. C. Schwartz, N. Shenoy, K. Shirasu, U. R. Sikhakolli, K. Stüber, S. A. Sukno, J. A. Sweigard, Y. Takano, H. Takahara, F. Trail, H. C. van der Does, L. M. Voll, I. Will, S. Young, Q. Zeng, J. Zhang, S. Zhou, M. B. Dickman, P. Schulze-Lefert, E. Ver Loren van Themaat, L. J. Ma, L. J. Vaillancourt, Lifestyle transitions in plant pathogenic Colletotrichum fungi deciphered by genome and transcriptome analyses. *Nat Genet* **44**, 1060-1065 (2012).
25. A. G. McLennan, The Nudix hydrolase superfamily. *Cell. Mol. Life Sci.* **63**, 123-143 (2006).
26. S. T. Safrany, S. W. Ingram, J. L. Cartwright, J. R. Falck, A. G. McLennan, L. D. Barnes, S. B. Shears, The diadenosine hexaphosphate hydrolases from *Schizosaccharomyces pombe* and *Saccharomyces cerevisiae* are homologues of the human diphosphoinositol polyphosphate phosphohydrolase: overlapping substrate specificities in a MutT-type protein. *J. Biol. Chem.* **274**, 21735-21740 (1999).
27. E. Grudzien-Nogalska, X. Jiao, M. G. Song, R. P. Hart, M. Kiledjian, Nudt3 is an mRNA decapping enzyme that modulates cell migration. *RNA* **22**, 773-781 (2016).
28. S. T. Safrany, J. J. Caffrey, X. Yang, M. E. Bembenek, M. B. Moyer, W. A. Burkhart, S. B. Shears, A novel context for the 'MutT'module, a guardian of cell integrity, in a diphosphoinositol polyphosphate phosphohydrolase. *EMBO J.* **17**, 6599-6607 (1998).
29. G. Zong, N. Jork, S. Hostachy, D. Fiedler, H. J. Jessen, S. B. Shears, H. Wang, New structural insights reveal an expanded reaction cycle for inositol pyrophosphate hydrolysis by human DIPP1. *FASEB J.* **35**, e21275 (2021).
30. C. L. McCombe, A. M. Catanzariti, J. R. Greenwood, A. M. Desai, M. A. Outram, D. S. Yu, D. J. Ericsson, S. E. Brenner, P. N. Dodds, B. Kobe, D. A. Jones, S. J. Williams, A rust-fungus Nudix hydrolase effector decaps mRNA *in vitro* and interferes with plant immune pathways. *New Phytol.* **239**, 222-239 (2023).
31. C. H. Khang, R. Berruyer, M. C. Giraldo, P. Kankanala, S. Y. Park, K. Czymmek, S. Kang, B. Valent, Translocation of Magnaporthe oryzae effectors into rice cells and their subsequent cell-to-cell movement. *Plant Cell* **22**, 1388-1403 (2010).
32. M. C. Giraldo, Y. F. Dagdas, Y. K. Gupta, T. A. Mentlak, M. Yi, A. L. Martinez-Rocha, H. Saitoh, R. Terauchi, N. J. Talbot, B. Valent, Two distinct secretion systems facilitate tissue invasion by the rice blast fungus Magnaporthe oryzae. *Nat. Commun.* **4**, 1996 (2013).
33. P. Chardin, F. McCormick, Brefeldin A: the advantage of being uncompetitive. *Cell* **97**, 153-155 (1999).
34. K. Duan, K. Yi, L. Dang, H. Huang, W. Wu, P. Wu, Characterization of a sub-family of Arabidopsis genes with the SPX domain reveals their diverse functions in plant tolerance to phosphorus starvation. *Plant J.* **54**, 965-975 (2008).
35. A. E. Angkawijaya, Y. Nakamura, Arabidopsis PECP1 and PS2 are phosphate starvation-inducible phosphocholine phosphatases. *Biochem. Biophys. Res. Commun.* **494**, 397-401 (2017).
36. M. Stegmann, J. Monaghan, E. Smakowska-Luzan, H. Rovenich, A. Lehner, N. Holton, Y. Belkhadir, C. Zipfel, The receptor kinase FER is a RALF-regulated scaffold controlling plant immune signaling. *Science* **355**, 287-289 (2017).
37. M. Paries, C. Gutjahr, The good, the bad, and the phosphate: regulation of beneficial and detrimental plant-microbe interactions by the plant phosphate status. *New Phytol.* **239**, 29-46 (2023).
38. K. Hiruma, N. Gerlach, S. Sacristán, R. T. Nakano, S. Hacquard, B. Kracher, U. Neumann, D. Ramírez, M. Bucher, R. J. O'Connell, P. Schulze-Lefert, Root Endophyte Colletotrichum tofieldiae Confers Plant Fitness Benefits that Are Phosphate Status Dependent. *Cell* **165**, 464-474 (2016).
39. S. Hacquard, B. Kracher, K. Hiruma, P. C. Münch, R. Garrido-Oter, M. R. Thon, A. Weimann, U. Damm, J. F. Dallery, M. Hainaut, B. Henrissat, O. Lespinet, S. Sacristán, E. Ver Loren van Themaat, E. Kemen, A.

C. McHardy, P. Schulze-Lefert, R. J. O'Connell, Survival trade-offs in plant roots during colonization by closely related beneficial and pathogenic fungi. *Nat. Commun.* **7**, 11362 (2016).
40. I. Fabiańska, N. Gerlach, J. Almario, M. Bucher, Plant-mediated effects of soil phosphorus on the root-associated fungal microbiota in Arabidopsis thaliana. *New Phytol.* **221**, 2123-2137 (2019).
41. O. M. Finkel, I. Salas-González, G. Castrillo, S. Spaepen, T. F. Law, P. Teixeira, C. D. Jones, J. L. Dangl, The effects of soil phosphorus content on plant microbiota are driven by the plant phosphate starvation response. *PLoS Biol.* **17**, e3000534 (2019).
42. R. J. Morcillo, S. K. Singh, D. He, G. An, J. I. Vílchez, K. Tang, F. Yuan, Y. Sun, C. Shao, S. Zhang, Y. Yang, X. Liu, Y. Dang, W. Wang, J. Gao, W. Huang, M. Lei, C. P. Song, J. K. Zhu, A. P. Macho, P. W. Paré, H. Zhang, Rhizobacterium-derived diacetyl modulates plant immunity in a phosphate-dependent manner. *EMBO J.* **39**, e102602 (2020).
43. P. L. Plaumann, J. Schmidpeter, M. Dahl, L. Taher, C. Koch, A Dispensable Chromosome Is Required for Virulence in the Hemibiotrophic Plant Pathogen Colletotrichum higginsianum. *Front Microbiol* **9**, 1005 (2018).
44. J. F. Dallery, N. Lapalu, A. Zampounis, S. Pigné, I. Luyten, J. Amselem, A. H. J. Wittenberg, S. Zhou, M. V. de Queiroz, G. P. Robin, A. Auger, M. Hainaut, B. Henrissat, K. T. Kim, Y. H. Lee, O. Lespinet, D. C. Schwartz, M. R. Thon, R. J. O'Connell, Gapless genome assembly of Colletotrichum higginsianum reveals chromosome structure and association of transposable elements with secondary metabolite gene clusters. *BMC Genomics* **18**, 667 (2017).
45. L. B. Sheard, X. Tan, H. Mao, J. Withers, G. Ben-Nissan, T. R. Hinds, Y. Kobayashi, F. F. Hsu, M. Sharon, J. Browse, S. Y. He, J. Rizo, G. A. Howe, N. Zheng, Jasmonate perception by inositol-phosphate-potentiated COI1-JAZ co-receptor. *Nature* **468**, 400-405 (2010).
46. D. Laha, N. Parvin, M. Dynowski, P. Johnen, H. Mao, S. T. Bitters, N. Zheng, G. Schaaf, Inositol Polyphosphate Binding Specificity of the Jasmonate Receptor Complex. *Plant Physiol.* **171**, 2364-2370 (2016).
47. X. Tan, L. I. Calderon-Villalobos, M. Sharon, C. Zheng, C. V. Robinson, M. Estelle, N. Zheng, Mechanism of auxin perception by the TIR1 ubiquitin ligase. *Nature* **446**, 640-645 (2007).
48. N. P. Laha, R. F. H. Giehl, E. Riemer, D. Qiu, N. J. Pullagurla, R. Schneider, Y. W. Dhir, R. Yadav, Y. E. Mihiret, P. Gaugler, V. Gaugler, H. Mao, N. Zheng, N. von Wirén, A. Saiardi, S. Bhattacharjee, H. J. Jessen, D. Laha, G. Schaaf, INOSITOL (1,3,4) TRIPHOSPHATE 5/6 KINASE1-dependent inositol polyphosphates regulate auxin responses in Arabidopsis. *Plant Physiol.* **190**, 2722-2738 (2022).
49. D. Laha, P. Johnen, C. Azevedo, M. Dynowski, M. Weiß, S. Capolicchio, H. Mao, T. Iven, M. Steenbergen, M. Freyer, P. Gaugler, M. K. de Campos, N. Zheng, I. Feussner, H. J. Jessen, S. C. Van Wees, A. Saiardi, G. Schaaf, VIH2 Regulates the Synthesis of Inositol Pyrophosphate InsP8 and Jasmonate-Dependent Defenses in Arabidopsis. *Plant Cell* **27**, 1082-1097 (2015).
50. G. A. Khan, E. Vogiatzaki, G. Glauser, Y. Poirier, Phosphate Deficiency Induces the Jasmonate Pathway and Enhances Resistance to Insect Herbivory. *Plant Physiol.* **171**, 632-644 (2016).
51. K. He, J. Du, X. Han, H. Li, M. Kui, J. Zhang, Z. Huang, Q. Fu, Y. Jiang, Y. Hu, PHOSPHATE STARVATION RESPONSE1 (PHR1) interacts with JASMONATE ZIM-DOMAIN (JAZ) and MYC2 to modulate phosphate deficiency-induced jasmonate signaling in Arabidopsis. *Plant Cell* **35**, 2132-2156 (2023).
52. E. Oliveira-Garcia, T. M. Tamang, J. Park, M. Dalby, M. Martin-Urdiroz, C. Rodriguez Herrero, A. H. Vu, S. Park, N. J. Talbot, B. Valent, Clathrin-mediated endocytosis facilitates the internalization of Magnaporthe oryzae effectors into rice cells. *Plant Cell* **35**, 2527-2551 (2023).
53. A. Wegner, F. Casanova, M. Loehrer, A. Jordine, S. Bohnert, X. Liu, Z. Zhang, U. Schaffrath, Gene deletion and constitutive expression of the pectate lyase gene 1 (MoPL1) lead to diminished virulence of Magnaporthe oryzae. *J. Microbiol.* **60**, 79-88 (2022).
54. F. Teufel, J. J. Almagro Armenteros, A. R. Johansen, M. H. Gíslason, S. I. Pihl, K. D. Tsirigos, O. Winther, S. Brunak, G. von Heijne, H. Nielsen, SignalP 6.0 predicts all five types of signal peptides using protein language models. *Nat. Biotechnol.* **40**, 1023-1025 (2022).
55. A. R. Bentham, M. Youles, M. N. Mendel, F. A. Varden, J. C. D. l. Concepcion, M. J. Banfield, pOPIN-GG: A resource for modular assembly in protein expression vectors. *bioRxiv*, 2021.2008.2010.455798 [Preprint] (2021). https://doi.org/10.1101/2021.08.10.455798.
56. E. Weber, C. Engler, R. Gruetzner, S. Werner, S. Marillonnet, A modular cloning system for standardized assembly of multigene constructs. *PLoS One* **6**, e16765 (2011).
57. F. W. Studier, Protein production by auto-induction in high density shaking cultures. *Protein Expr. Purif.* **41**, 207-234 (2005).

58. E. W. Sayers, E. E. Bolton, J. R. Brister, K. Canese, J. Chan, D. C. Comeau, C. M. Farrell, M. Feldgarden, A. M. Fine, K. Funk, E. Hatcher, S. Kannan, C. Kelly, S. Kim, W. Klimke, M. J. Landrum, S. Lathrop, Z. Lu, T. L. Madden, A. Malheiro, A. Marchler-Bauer, T. D. Murphy, L. Phan, S. Pujar, S. H. Rangwala, V. A. Schneider, T. Tse, J. Wang, J. Ye, B. W. Trawick, K. D. Pruitt, S. T. Sherry, Database resources of the national center for biotechnology information in 2023. *Nucleic Acids Res.* **51**, D29-D38 (2023).
59. M. Blum, H. Y. Chang, S. Chuguransky, T. Grego, S. Kandasaamy, A. Mitchell, G. Nuka, T. Paysan-Lafosse, M. Qureshi, S. Raj, L. Richardson, G. A. Salazar, L. Williams, P. Bork, A. Bridge, J. Gough, D. H. Haft, I. Letunic, A. Marchler-Bauer, H. Mi, D. A. Natale, M. Necci, C. A. Orengo, A. P. Pandurangan, C. Rivoire, C. J. A. Sigrist, I. Sillitoe, N. Thanki, P. D. Thomas, S. C. E. Tosatto, C. H. Wu, A. Bateman, R. D. Finn, The InterPro protein families and domains database: 20 years on. *Nucleic Acids Res.* **49**, D344-D354 (2021).
60. S. Guindon, J. F. Dufayard, V. Lefort, M. Anisimova, W. Hordijk, O. Gascuel, New algorithms and methods to estimate maximum-likelihood phylogenies: assessing the performance of PhyML 3.0. *Syst. Biol.* **59**, 307-321 (2010).
61. I. Letunic, P. Bork, Interactive Tree Of Life (iTOL) v5: an online tool for phylogenetic tree display and annotation. *Nucleic Acids Res.* **49**, W293-W296 (2021).
62. A. Heese, D. R. Hann, S. Gimenez-Ibanez, A. M. E. Jones, K. He, J. Li, J. I. Schroeder, S. C. Peck, J. P. Rathjen, The receptor-like kinase SERK3/BAK1 is a central regulator of innate immunity in plants. *Proc. Natl. Acad. Sci. U S A* **104**, 12217-12222 (2007).
63. R. Puschmann, R. K. Harmel, D. Fiedler, Scalable Chemoenzymatic Synthesis of Inositol Pyrophosphates. *Biochemistry* **58**, 3927-3932 (2019).
64. O. Loss, C. Azevedo, Z. Szijgyarto, D. Bosch, A. Saiardi, Preparation of quality inositol pyrophosphates. *JoVE* **55**, e3027 (2011).
65. D. Aragão, J. Aishima, H. Cherukuvada, R. Clarken, M. Clift, N. P. Cowieson, D. J. Ericsson, C. L. Gee, S. Macedo, N. Mudie, MX2: a high-flux undulator microfocus beamline serving both the chemical and macromolecular crystallography communities at the Australian Synchrotron. *Journal of synchrotron radiation* **25**, 885-891 (2018).
66. W. Kabsch, XDS. *Acta Crystallogr. D Biol. Crystallogr.* **66**, 125-132 (2010).
67. P. R. Evans, G. N. Murshudov, How good are my data and what is the resolution? *Acta Crystallogr. D Biol. Crystallogr.* **69**, 1204-1214 (2013).
68. D. Liebschner, P. V. Afonine, M. L. Baker, G. Bunkóczi, V. B. Chen, T. I. Croll, B. Hintze, L.-W. Hung, S. Jain, A. J. McCoy, Macromolecular structure determination using X-rays, neutrons and electrons: recent developments in Phenix. *Acta Crystallogr. D Struct. Biol.* **75**, 861-877 (2019).
69. J. Jumper, R. Evans, A. Pritzel, T. Green, M. Figurnov, O. Ronneberger, K. Tunyasuvunakool, R. Bates, A. Žídek, A. Potapenko, A. Bridgland, C. Meyer, S. A. A. Kohl, A. J. Ballard, A. Cowie, B. Romera-Paredes, S. Nikolov, R. Jain, J. Adler, T. Back, S. Petersen, D. Reiman, E. Clancy, M. Zielinski, M. Steinegger, M. Pacholska, T. Berghammer, S. Bodenstein, D. Silver, O. Vinyals, A. W. Senior, K. Kavukcuoglu, P. Kohli, D. Hassabis, Highly accurate protein structure prediction with AlphaFold. *Nature* **596**, 583-589 (2021).
70. T. C. Terwilliger, R. W. Grosse-Kunstleve, P. V. Afonine, N. W. Moriarty, P. H. Zwart, L.-W. Hung, R. J. Read, P. D. Adams, Iterative model building, structure refinement and density modification with the PHENIX AutoBuild wizard. *Acta Crystallogr. D Biol. Crystallogr.* **64**, 61-69 (2008).
71. A. Casañal, B. Lohkamp, P. Emsley, Current developments in Coot for macromolecular model building of Electron Cryo-microscopy and Crystallographic Data. *Protein Sci.* **29**, 1069-1078 (2020).
72. P. V. Afonine, R. W. Grosse-Kunstleve, N. Echols, J. J. Headd, N. W. Moriarty, M. Mustyakimov, T. C. Terwilliger, A. Urzhumtsev, P. H. Zwart, P. D. Adams, Towards automated crystallographic structure refinement with phenix. refine. *Acta Crystallogr. D Biol. Crystallogr.* **68**, 352-367 (2012).
73. E. F. Pettersen, T. D. Goddard, C. C. Huang, E. C. Meng, G. S. Couch, T. I. Croll, J. H. Morris, T. E. Ferrin, UCSF ChimeraX: Structure visualization for researchers, educators, and developers. *Protein Sci.* **30**, 70-82 (2021).
74. B. Yariv, E. Yariv, A. Kessel, G. Masrati, A. B. Chorin, E. Martz, I. Mayrose, T. Pupko, N. Ben-Tal, Using evolutionary data to make sense of macromolecules with a "face-lifted" ConSurf. *Protein Sci.* **32**, e4582 (2023).
75. J. Vandesompele, K. De Preter, F. Pattyn, B. Poppe, N. Van Roy, A. De Paepe, F. Speleman, Accurate normalization of real-time quantitative RT-PCR data by geometric averaging of multiple internal control genes. *Genome Biol.* **3**, research0034 (2002).

76. M. A. Pombo, R. N. Ramos, Y. Zheng, Z. Fei, G. B. Martin, H. G. Rosli, Transcriptome-based identification and validation of reference genes for plant-bacteria interaction studies using *Nicotiana benthamiana*. *Sci. Rep.* **9**, 1632 (2019).
77. J. Chen, M. Luo, P. Hands, V. Rolland, J. Zhang, Z. Li, M. Outram, P. Dodds, M. Ayliffe, A split GAL4 RUBY assay for visual in planta detection of protein-protein interactions. *Plant J.* **114**, 1209-1226 (2023).
78. D. Janus, B. Hoff, E. Hofmann, U. Kück, An efficient fungal RNA-silencing system using the DsRed reporter gene. *Appl. Environ. Microbiol.* **73**, 962-970 (2007).
79. P. Kankanala, K. Czymmek, B. Valent, Roles for rice membrane dynamics and plasmodesmata during biotrophic invasion by the blast fungus. *Plant Cell* **19**, 706-724 (2007).
80. S. Che Omar, M. A. Bentley, G. Morieri, G. M. Preston, S. J. Gurr, Validation of Reference Genes for Robust qRT-PCR Gene Expression Analysis in the Rice Blast Fungus Magnaporthe oryzae. *PLoS One* **11**, e0160637 (2016).
81. S. L. Ding, W. Liu, A. Iliuk, C. Ribot, J. Vallet, A. Tao, Y. Wang, M. H. Lebrun, J. R. Xu, The tig1 histone deacetylase complex regulates infectious growth in the rice blast fungus Magnaporthe oryzae. *Plant Cell* **22**, 2495-2508 (2010).
82. E. Oliveira-Garcia, B. Valent, Characterizing the Secretion Systems of Magnaporthe oryzae. *Methods Mol Biol* **2356**, 69-77 (2021).
83. X. L. Chen, T. Shi, J. Yang, W. Shi, X. Gao, D. Chen, X. Xu, J. R. Xu, N. J. Talbot, Y. L. Peng, N-glycosylation of effector proteins by an α-1,3-mannosyltransferase is required for the rice blast fungus to evade host innate immunity. *Plant Cell* **26**, 1360-1376 (2014).
84. A. Wegner, L. Wirtz, T. Leisen, M. Hahn, U. Schaffrath, Fenhexamid - an efficient and inexpensive fungicide for selection of Magnaporthe oryzae transformants. *European Journal of Plant Pathology* **162**, 697-707 (2022).
85. T. Leisen, F. Bietz, J. Werner, A. Wegner, U. Schaffrath, D. Scheuring, F. Willmund, A. Mosbach, G. Scalliet, M. Hahn, CRISPR/Cas with ribonucleoprotein complexes and transiently selected telomere vectors allows highly efficient marker-free and multiple genome editing in Botrytis cinerea. *PLoS Pathog* **16**, e1008326 (2020).
86. A. J. Foster, M. Martin-Urdiroz, X. Yan, H. S. Wright, D. M. Soanes, N. J. Talbot, CRISPR-Cas9 ribonucleoprotein-mediated co-editing and counterselection in the rice blast fungus. *Scientific Reports* **8**, 14355 (2018).
87. P. Virtanen, R. Gommers, T. E. Oliphant, M. Haberland, T. Reddy, D. Cournapeau, E. Burovski, P. Peterson, W. Weckesser, J. Bright, S. J. van der Walt, M. Brett, J. Wilson, K. J. Millman, N. Mayorov, A. R. J. Nelson, E. Jones, R. Kern, E. Larson, C. J. Carey, İ. Polat, Y. Feng, E. W. Moore, J. VanderPlas, D. Laxalde, J. Perktold, R. Cimrman, I. Henriksen, E. A. Quintero, C. R. Harris, A. M. Archibald, A. H. Ribeiro, F. Pedregosa, P. van Mulbregt, SciPy 1.0: fundamental algorithms for scientific computing in Python. *Nat Methods* **17**, 261-272 (2020).
88. M.-G. Song, Y. Li, M. Kiledjian, Multiple mRNA decapping enzymes in mammalian cells. *Molecular cell* **40**, 423-432 (2010).

Acknowledgments: We thank the Plant Services Team at the Australian National University for providing *N. benthamiana* seedlings, and all the Williams lab members for helpful discussion. The authors acknowledge the use of the ANU crystallization facility. The authors also acknowledge the use of the Australian Synchrotron MX facility and thank the staff for their support. This research was undertaken in part using the MX2 beamline at the Australian Synchrotron, part of ANSTO, and made use of the Australian Cancer Research Foundation (ACRF) detector. Fig. 5 and S8A were created with BioRender.com.

Funding:

Australian Institute of Nuclear Science and Engineering Ltd. Postgraduate Research Award (CLM)

Australian Government Research Training Programme Stipend (CLM)

ANU Future Scheme 35665 (SJW)

ARC Future Fellowship FT200100135 (SJW)

Louisiana Board of Regents grant #LEQSF (2022-24)-RD-A-01 (EOG)

RWTH Aachen University scholarships for Doctoral Students (AW, FC, LW)

Funded by the Deutsche Forschungsgemeinschaft (DFG, German Research Foundation) – 410278620 (US, AW)

Author contributions:

Conceptualization: CLM, AW, SJW, US

Methodology: CLM, AW, SA, JRG, EOG, SJW, US

Investigation: CLM, AW, CSZ, FC, SA, JRG, LW, SdP, EE, SS, EOG

Formal Analysis: CLM, AW, CSZ, FC, SA, DJE, EOG, SJW

Visualization: CLM, AW, CSZ, FC, SA, EOG

Funding acquisition: EOG, SJW, US

Project administration: CLM, AW, SJW, US

Supervision: CLM, AW, EOG, SJW, US

Writing – original draft: CLM, AW

Writing – review & editing: CLM, AW, FC, SA, JRG, LW, SS, EE, DJE, EOG, SJW, US

Competing interests: Authors declare that they have no competing interests.

Data and materials availability: Where possible all materials generated in this study will be made available upon request to the corresponding authors. The data that support the MoNUDIX protein structure described in this study are openly available under accession 8SXS at the PDB. All other data are available in the main text or supplementary materials.

Supplementary Materials

Materials and Methods

Figs. S1 to S8

Tables S1 to S6

References (*52–88*)

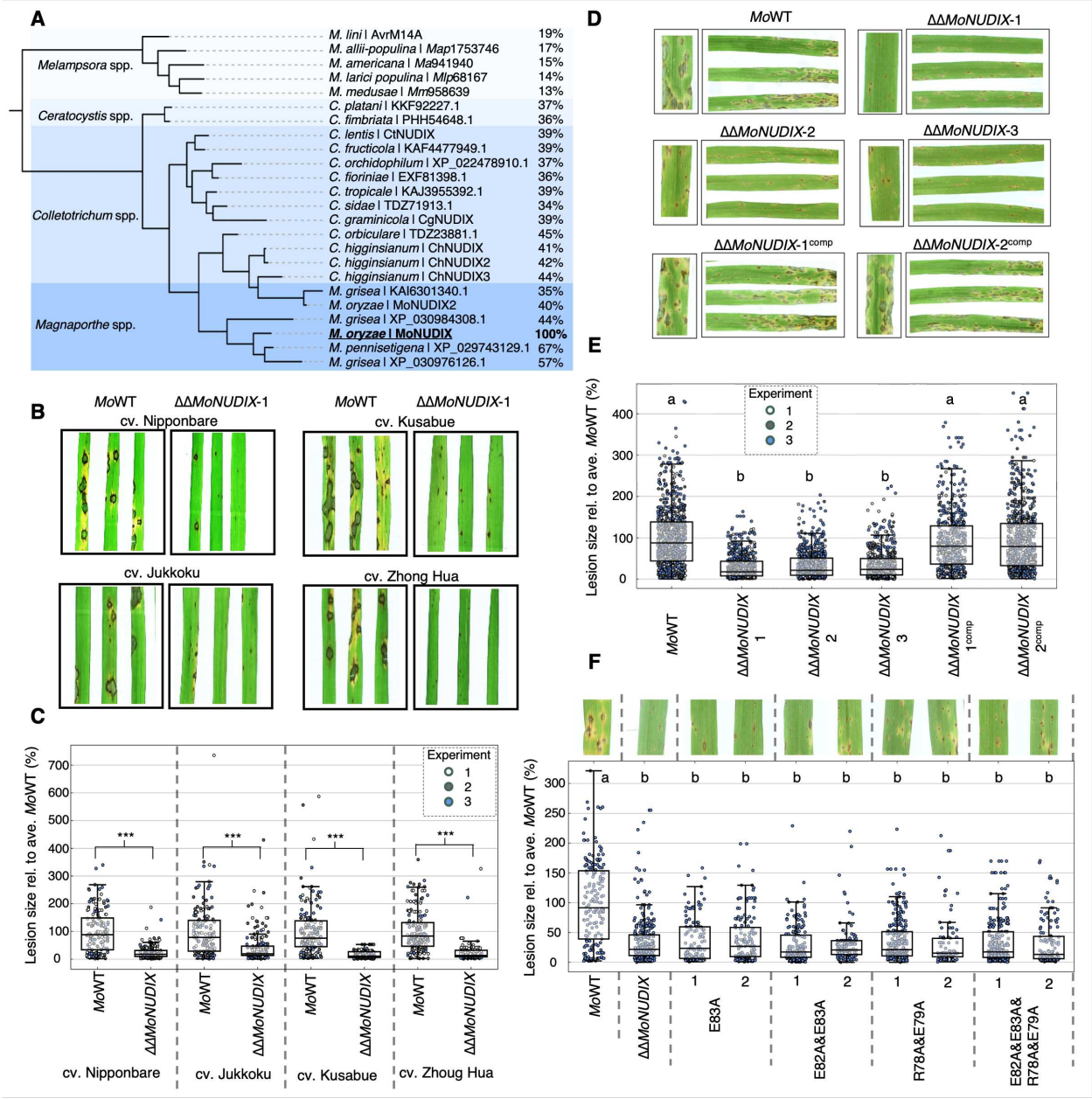

Fig. 1. MoNUDIX is important for *Magnaporthe oryzae* virulence on rice and barley.
(**A**) A phylogeny indicating the evolutionary relationships between Nudix hydrolase effectors from pathogenic fungi, the percentage value indicates amino acid sequence identity with MoNUDIX. (**B**) Rice cultivars Nipponbare, Jukkoku, Kusabue and Zhoug Hua were spray inoculated with *M. oryzae* isolate Guy11 (*Mo*WT) and *MoNUDIX* double gene deletion mutant Δ*MoNUDIX*-1. Leaves were photographed six days post inoculation (dpi). **(C)** Boxplots summarize the results of three independent experiments, with the size of approximately 50 lesions measured across 5 rice leaves per treatment. Asterisks indicate treatments on the same cultivar with significantly different lesion sizes (Mann-Whitney U test, $P < 0.001$). (**D**) The barley cultivar Ingrid was inoculated with *Mo*WT, Δ*MoNUDIX*-1, Δ*MoNUDIX*-2, Δ*MoNUDIX-3*, and MoNUDIX complementation mutants (Δ*MoNUDIX*-1^{comp} and Δ*MoNUDIX*-2^{comp}). Leaves were photographed seven dpi. (**E**) Boxplots summarize the results of three independent experiments with approximately 150 lesions

measured across 10 barley leaves per treatment. Letters depict significant differences between treatments (Kruskal-Wallis H test, Dunn's post-hoc test, $P < 0.01$). (**F**) The barley cultivar Ingrid was inoculated with *Mo*WT, Δ*MoNUDIX*-1, and Δ*MoNUDIX*-1 complemented with MoNUDIX variants harboring substitution mutations in the Nudix box motif. Two independent complementation lines were tested for each variant. Example images at seven dpi are displayed. Boxplots summarize the results, the size of approximately 150 lesions were measured across 10 barley leaves. Letters depict significant differences between treatments (Kruskal-Wallis H test, Dunn's post-hoc test, $P < 0.01$).

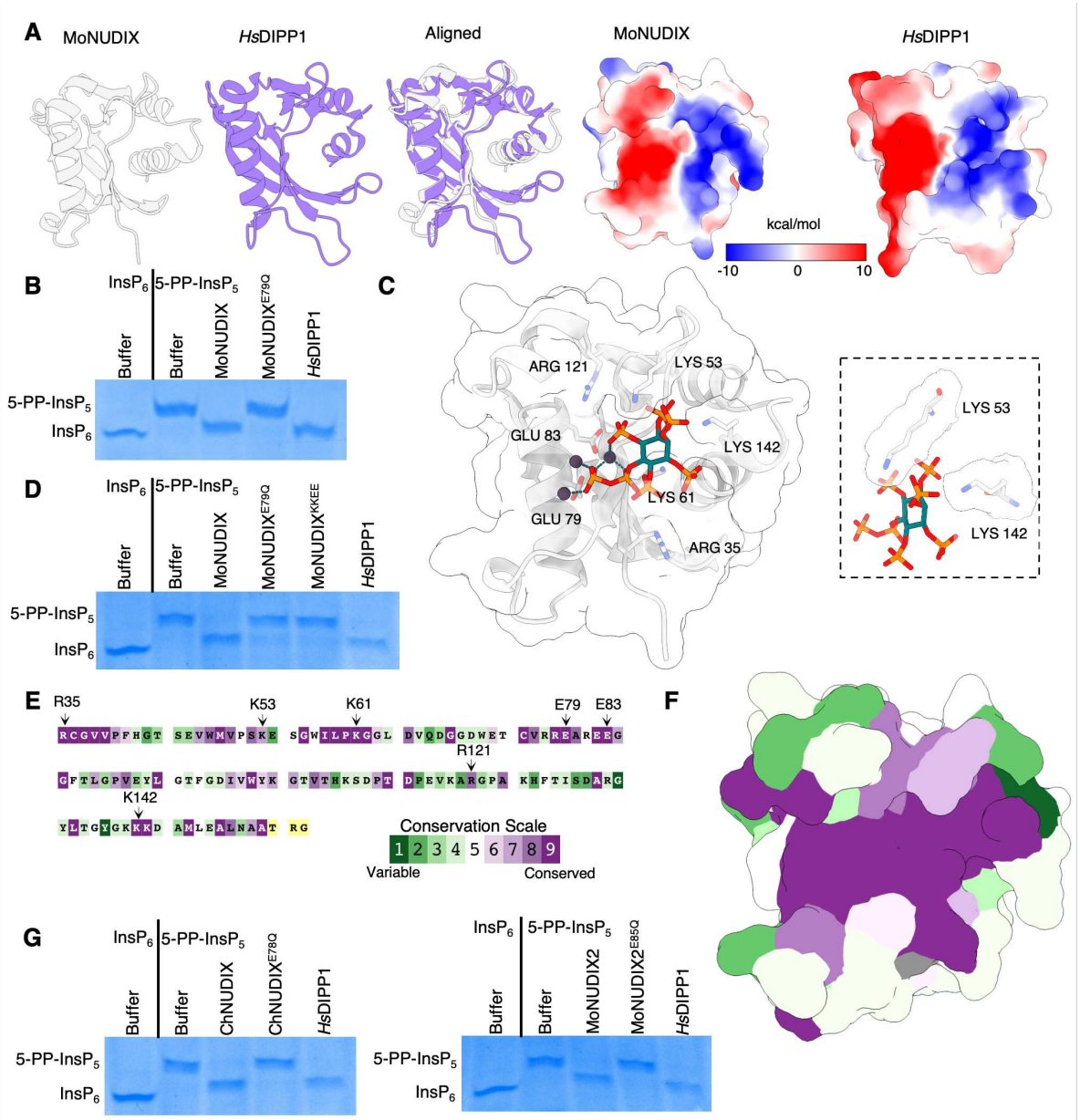

Fig. 2. *Magnaporthe* and *Colletotrichum* Nudix effectors are diphosphoinositol polyphosphate phosphohydrolases.

(**A**) MoNUDIX and *Homo sapiens* DIPP1 (PDB: 6WO7) (*26*) crystal structures superimposed to demonstrate their structural similarity despite low levels of sequence identity (25%). (Right) Both MoNUDIX and *Hs*DIPP1 demonstrate similar surface charge properties at the putative active site. (**B**) Purified MoNUDIX, MoNUDIX^{E79Q}, and *Hs*DIPP1 were incubated with 5-PP-InsP$_5$. Buffer alone was incubated with both InsP$_6$ and 5-PP-InsP$_5$. The reaction products were separated using a polyacrylamide gel and stained with toluidine blue. (**C**) MoNUDIX with Mg^{2+} and 5-PP-InsP$_5$ docked into the crystal structure via alignment with *Hs*DIPP1 (PDB: 6WO7). The amino acids potentially important for Mg^{2+} and 5-PP-InsP$_5$ binding are labelled. In the box are the two lysine amino acids selected for mutagenesis. (**D**) Inositol pyrophosphate hydrolysis assays demonstrate the importance of lysine 53 and 142. (**E**) The sequence of MoNUDIX used to determine the crystal structure, with colouring indicating amino acid conservation across homologous effectors. The

amino acids labelled in (**C**) are indicated with arrows. (**F**) MoNUDIX with the protein surface coloured according to amino acid conservation across homologous effectors, demonstrating high conservation of the putative substrate binding site. (**G**) Inositol pyrophosphate hydrolysis assays with MoNUDIX homologs ChNUDIX and MoNUDIX2 demonstrates Nudix motif-dependent hydrolysis of 5-PP-InsP_5.

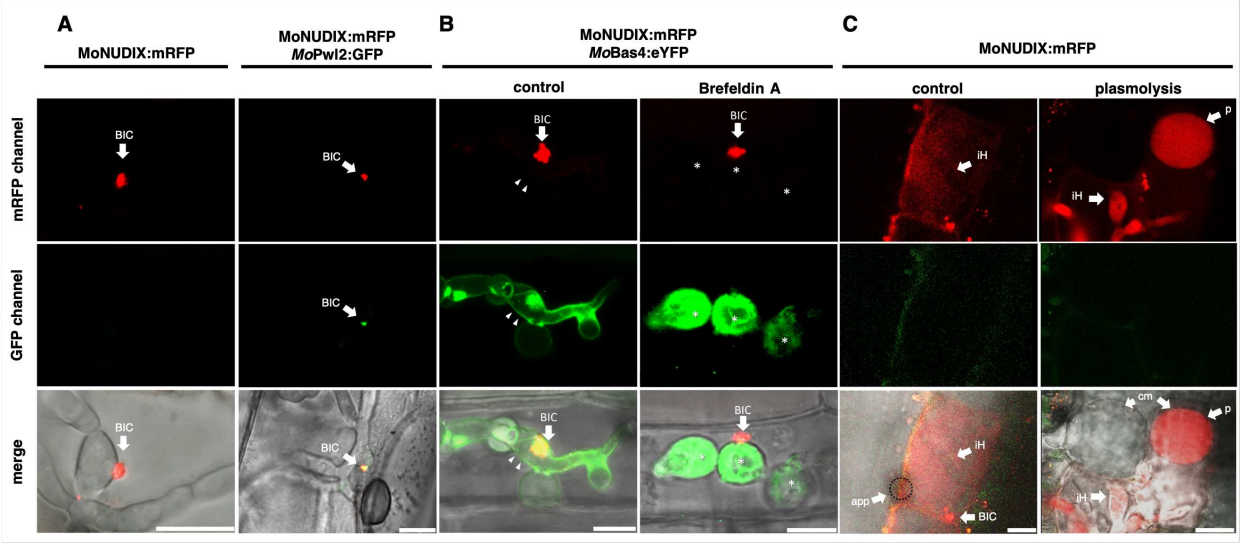

Fig. 3. MoNUDIX localizes to the biotrophic interfacial complex and is secreted into the host cytoplasm during infection.

Confocal laser-scanning microscopy images of barley and rice leaves infected with *Magnaporthe oryzae* expressing fluorescent protein-tagged effectors. (**A**) (Left) Barley leaves were inoculated with *M. oryzae* expressing MoNUDIX:mRFP. At 48 hours post inoculation (hpi), punctual accumulation of the mRFP fusion protein in the fungal hyphae was observed in the first infected cell, consistent with BIC localization. (Right) The cytoplasmic effector *Mo*Pwl2 *(27)* was co-expressed as a GFP-fusion protein demonstrating co-localization of MoNUDIX:mRFP and *Mo*Pwl2:GFP. (**B**) Rice leaves were inoculated with *M. oryzae* expressing MoNUDIX:mRFP and *Mo*Bas4:eYFP. *Mo*Bas4:eYFP (green) shows apoplastic localization outlining the invasive hypha (arrowheads). In the presence of BFA, *Mo*Bas4:eYFP (green) is retained in the fungal ER (asterisks), but MoNUDIX:mRFP remains BIC-localized (arrow), imaged with the same transformant at 3 h after exposure to BFA. **(C)** Secretion of MoNUDIX into the rice cell cytoplasm. Rice leaves were inoculated with *M. oryzae* expressing MoNUDIX:mRFP and analyzed 48 hpi. For concentration of the intracellular mRFP signal we used plasmolysis with 0.5 M KNO_3 prior to imaging; BIC: biotrophic interfacial complex; iH: invasive hyphae; p: rice protoplast after plasmolysis; i: infected cell; cm: cell membrane of protoplast. Scale bar: 10 µm.

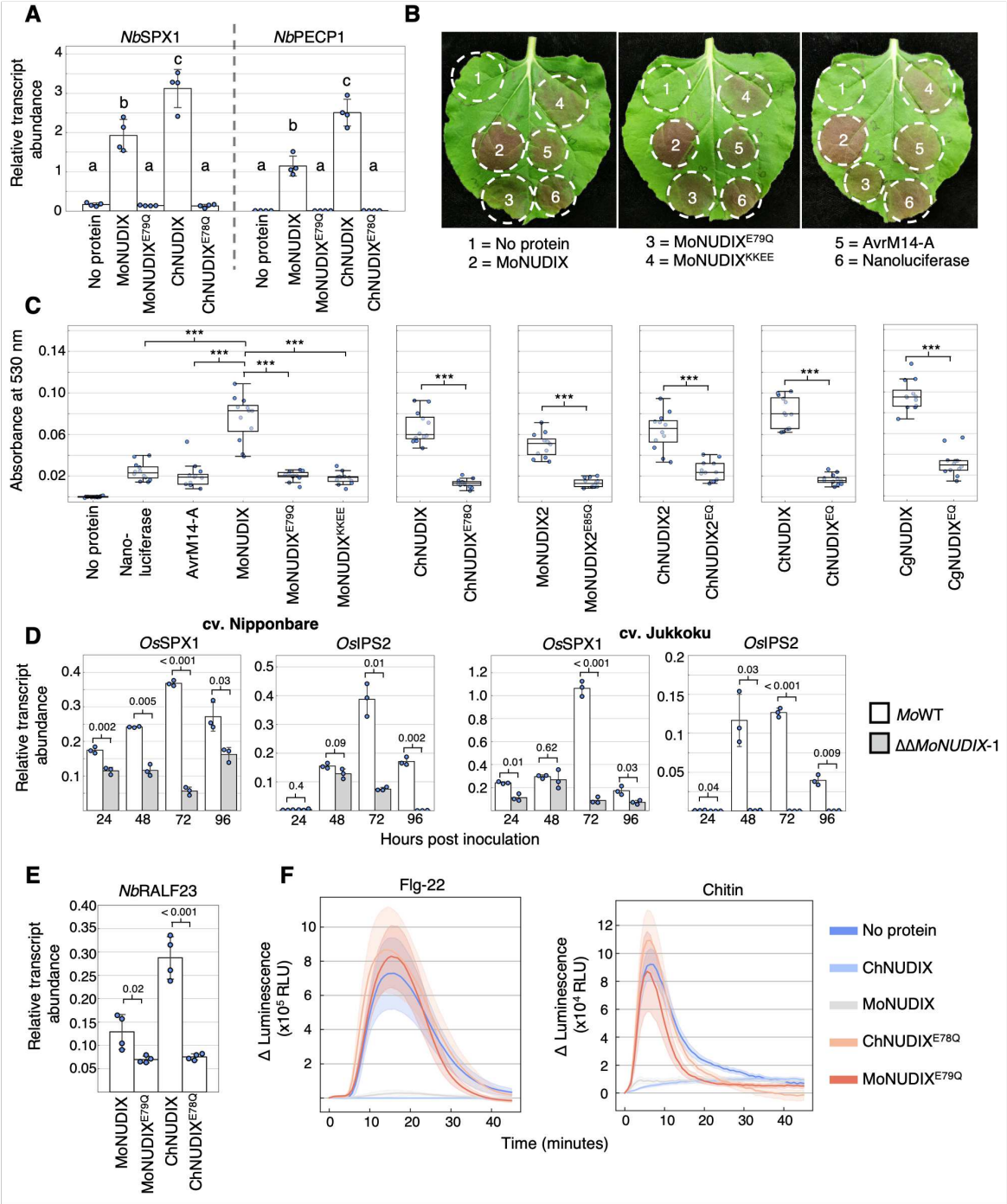

Fig. 4. The Nudix effector family activates plant phosphate starvation responses.
(**A**) The transcript abundance of *Nb*SPX1 and *Nb*PECP1 in *N. benthamiana* expressing Nudix effectors, or leaves transformed with an empty vector control (no protein). Values are mean expression ± SD (n = 4) relative to the reference genes, letters indicate significantly different groups (one-way ANOVA, Tukey's HSD, $P < 0.001$). (**B**) Visible RUBY production in leaves co-transformed with PSI:RUBY and Nudix effectors or controls. (**C**) The absorbance of extracts from leaves co-transformed with PSI:RUBY and Nudix effectors or controls (n = 12), asterisks indicate significant differences between treatments (one-way ANOVA, Tukey's HSD, *** $P < 0.001$). (**D**)

Rice cultivars Nipponbare and Jukkoku were inoculated with *M. oryzae* isolate Guy11 (*Mo*WT) and *M. oryzae*$^{\Delta\Delta MoNUDIX\text{-}1}$. *Os*SPX1 and *Os*IPS2 transcript abundance was calculated relative to *Os*ACTIN at four timepoints throughout the infection process, values are mean ± SD (n = 3), significant differences between *Mo*WT and ΔΔ*MoNUDIX*-1 treatments were identified by an independent samples t test, p-values are listed. (**E**) The expression of *Nb*RALF23 in *N. benthamiana* leaves expressing Nudix proteins (as labelled). Values are mean ± SD (n=4) relative to the reference genes, with p-values from an independent samples t-test displayed. (**F**) Reactive oxygen species production in *N. benthamiana* expressing Nudix effectors, or leaves transformed with an empty vector control (no protein), following exposure to flg-22 (left) or chitin (right). Values are mean (solid line) ± SEM (shaded area) (n = 8).

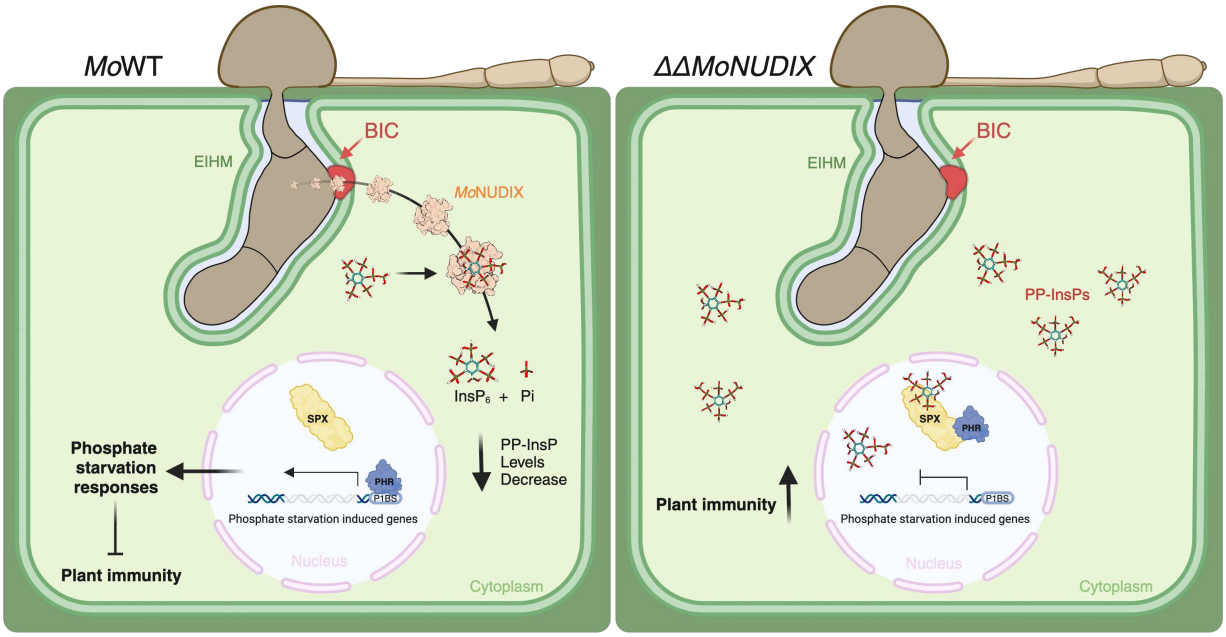

Fig. 5. A model for the virulence function of the *Magnaporthe* and *Colletotrichum* Nudix hydrolase effectors. (Left) In wild-type *M. oryzae* (*Mo*WT) MoNUDIX is secreted from the invading fungus into the host cell cytoplasm. MoNUDIX functions as an enzyme, hydrolyzing inositol pyrophosphate (PP-InsP) signaling molecules into inositol hexakisphosphate ($InsP_6$) and phosphate (Pi). The decrease in PP-InsP concentration prevents SPX-mediated inhibition of PHRs, resulting in the transcription of phosphate starvation inducible genes. Phosphate starvation responses are therefore activated, including those which suppress plant immune responses. (Right) Without MoNUDIX, the ability of *M. oryzae*$^{\Delta\Delta MoNUDIX}$ to stimulate PP-InsP hydrolysis is compromised. Available PP-InsPs are detected by SPX domains, resulting in the binding of SPX domains to PHRs. This prevents PHRs from binding to the P1BS elements in phosphate starvation induced genes. In the absence of phosphate starvation signaling, plant immune responses are prioritized.